

INVESTIGATION OF DISSIMILAR LASER WELDING OF STAINLESS STEEL 316L TO ALUMINIUM A1050 IN LAP JOINTS CONFIGURATION

Diana CHIOIBAŞU^{1,2}, Bogdan CĂLIN^{1,2}, Andrei POPESCU¹, Nicolae PUŞCAŞ², Damjan KLOBČAR³

A continuous wave fibre laser was applied in lap joint configuration in order to weld 1 mm thick stainless steel to 1 mm thick aluminium, with the stainless steel on the top. The laser system was used at maximum power to ensure full penetration depth. In order to produce pore free and aesthetic welds, other processing parameters were optimized, such laser velocity and focusing position. The dissimilar joints were studied by optical metallography, scanning electron microscopy and mechanically evaluated by pull-out tests. The potential of this joining method is discussed, based on the results of the analysis.

Keywords: dissimilar SS - Al welding; fibre laser welding; lap joint configuration; tensile strength.

1. Introduction

The advance of laser material processing is widely discussed in recent years. Investigations of laser processing we conducted in many areas of research, as well as for industrial applications. Among these we can mention laser ablation [1] [2] [3], laser cutting [4], laser welding [5], laser metal deposition [6], and others.

Steel-aluminium welding is already used in car construction for several reasons, such as reducing overall material quantity, therefore reducing CO₂ emissions and fuel consumption implicitly. Fibre laser welding of dissimilar aluminium-steel joints are of interest for such applications. A metallography analysis-based joining method, as well as tensile tests reaching strengths of up to 120 MPa, were reported [7]. Investigations on dissimilar laser beam welding of steel HX220LAD+Z100, 22MnB5+AS150, 1.4301 and aluminium alloy AA6016-T4 in lap joint configuration were established. These investigations were conducted after tensile tests and metallography evaluation depending on the energy per unit

¹ Center for Advanced Laser Technologies (CETAL), National Institute for Laser, Plasma and Radiation Physics, Magurele, Bucharest, RO-077125, Romania

² University POLITEHNICA of Bucharest, Doctoral School of the Faculty of Applied Science, Splaiul Independentei 313, Bucharest, RO-060042, Romania

³ University of Ljubljana, Faculty of Mechanical Engineering, Aškerčeva 6, 1000 Ljubljana, Slovenia

length [8]. Parameter optimization in laser welding is crucial to the process. Generic Algorithm Optimized Back Propagation Neural Network (GA-BPNN) has been used as an optimization method. This demonstrated the relationship between the weld bead integrity and process parameters [9].

This paper focuses on the study of defects in laser welding of stainless steel 316L and aluminium alloy A1050. The analysis is conducted through the variation of laser speed and focus position. The weld shape was examined from a metallographic point of view, while mechanical properties were determined by subjecting the samples to a series of tensile tests.

2. Materials and experimental set-up

2.1 Materials

The physical properties and chemical characteristics of the two materials which were used for dissimilar welding are presented in Table 1. The materials used for the investigations are 316L steel and A1050 aluminium. The size of the sample for each material are 80mm x 40mm, and a thickness of 1mm. In order to obtain better quality welding, the surface of each sample was cleaned with alcohol and dried in warm air. The samples were positioned with an overlap of 20 mm in order to perform tensile tests.

Table 1

Properties of AISI 316L stainless steel and aluminum alloy A1050

Material	AISI 316 L	A 1050
Melting point (°C)	1400	650
Thermal conductivity (W/m.K)	16.2	222
Relative density (g/cm ³)	7.99	0.00271
Hardness (HB)	95 (Rockwell)	34 (Brinell)
Modulus of elasticity (GPa)	200	71
Rm (MPa)	485	145

2.2 Experimental set-up

An Yt:YAG fiber laser was used for welding experiments, with a maximum power of 400 W in continuous mode (IPG Photonics, model YLR-400-AC,

wavelength 1070 nm). A three-dimensional scanning head (HighYAG, RLSK) with a 500 mm focus point lens was attached to a six axis robot machinery (Motoman MC2000). Furthermore, the scanning head has two mirrors that directs the laser beam in X and Y direction.

Focus position can change in Z direction (± 100 mm) by moving the collimating lens inside of the head. The laser spot diameter was $70 \mu\text{m}$ in the focus position. In order to absorb part of the heat due to the laser processing, a copper backing plate was placed under the working pieces during the welding process. The laser equipment is presented in the Fig. 1.

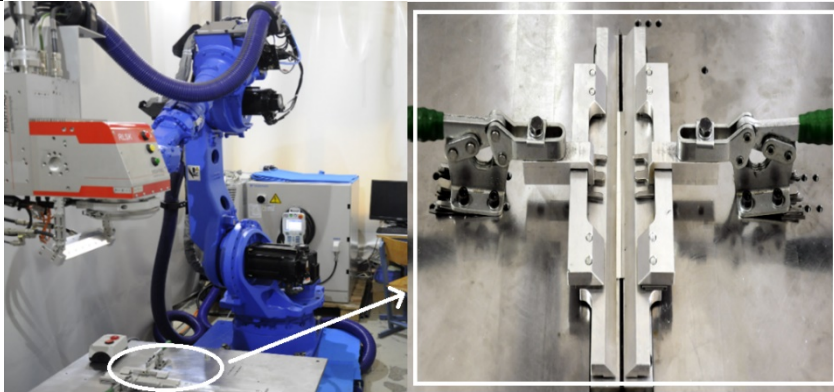


Fig. 1. Equipment and experimental set-up for the laser welding of dissimilar materials.

Argon shielding gas was used to create a protective atmosphere around the weld. The gas was used for shielding above and below the sample, with a 7 l/min debit. The clamping system was made of two vices, which prevents deformations that might occur after the welding process is completed. The materials were welded in a lap joint configuration with the steel over the aluminium. This configuration was chosen because the aluminium surface is easily oxidized and the reflectivity of the laser is high.

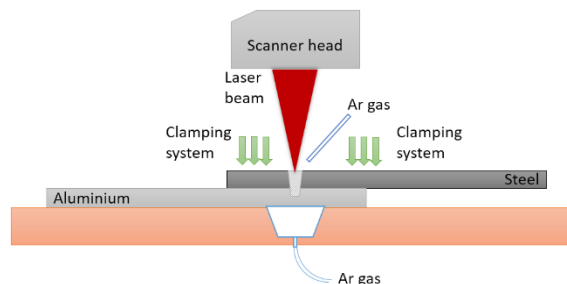


Fig. 2. Schematic representation of the laser welding process in lap-joint configuration. 2.3 Laser welding experiments.

These lead to a low absorption rate of aluminium. Moreover, the oxide is difficult to weld and defects can occur, such as inclusions and porosity. A schematic representation of the welding process is presented in the Fig. 2.

The experiments were conducted using a constant laser power at 400 W, while changing the focus position and velocity. Negative focus position means the focus is inside the sample. A total of 12 experiments were done in order to establish the effect of the focus position and the laser speed. Parameters are shown in Table 2. Experimental results were used to identify the optimal parameters necessary to obtain good welds.

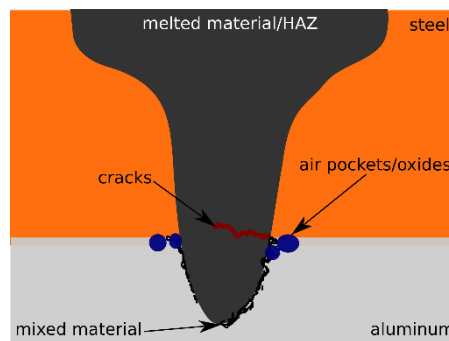


Fig. 3. Schematic representation of the main characteristics encountered in lap-joint welds

Table 2

Processing parameters

No.	Speed (m/min)	Focus (mm)
1	0.5	0
2	0.5	-1
3	0.5	-2
4	0.3	0
5	0.3	-1
6	0.3	-2
7	0.2	0
8	0.2	-2
9	0.4	0
10	0.4	-2
11	0.2/45°	0
12	3	0

3 Results and analysis

3.1 Metallographic analysis

The metallographic analysis of cross-sections consists in the examination of defect development and the effects produced by the variation of processing parameters. After polishing, Carpenter 300 series stainless steel etchant was used to show the bead shape. Weld shape and penetration depth were evaluated using an optical microscope for all the samples (Olympus Inverted Metallurgical Microscope GX 51, connected to a camera, Leica DFC 295). A schematic representation of weld characteristics is presented in figure 3, while experimental results are presented in figure 4. The heat affected zone (HAZ) can be easily observed from the metallographic analysis of the cross-sections. HAZ extends around the welded area almost within the same dimensions.

The HAZ varies with both laser power and scanning speed. Results show that the HAZ is larger for higher scanning speeds. We attribute this effect to fluid movements of the melted pool, as well as the plasma resulted from the laser-matter interaction. To advance this hypothesis, using low processing speeds results in a larger quantity of melted material due to a higher energy dose delivered to the material. The energy transfer from the incident laser beam to the sample is mediated by turbulent flow of the melted material in the interaction volume. The volume of melted material advances in the same direction of the laser beam. This direction is strongly influenced by the pressure generated by the plasma, at the surface of the melted material. Using higher processing speeds results in shorter duration for the pressure applied on the melted material, which further determines a lower and less directional penetration of melted material. The energy is still dissipated as heat, therefore resulting in a wider HAZ.

3.2 Tensile strength

Results of the tensile strength tests are presented below. Tensile strength testing was applied on 3 samples: one welded without any crack and pores (figure 4.3), one with a few defects (figure 4.7) and one with many cracks (figure 4.8). The specimens were cut with sand jet into the shape presented in figure 5, according to EN ISO 15614-1:2004 "Specification and qualification of welding procedures for metallic materials". The tensile testing machine used for tensile strength was Zwick Z250. The procedure was performed at the room temperature 23 °C, with 100 N preload force, 0.0025 1/s speed in the yield range and 0.008 1/s test speed.

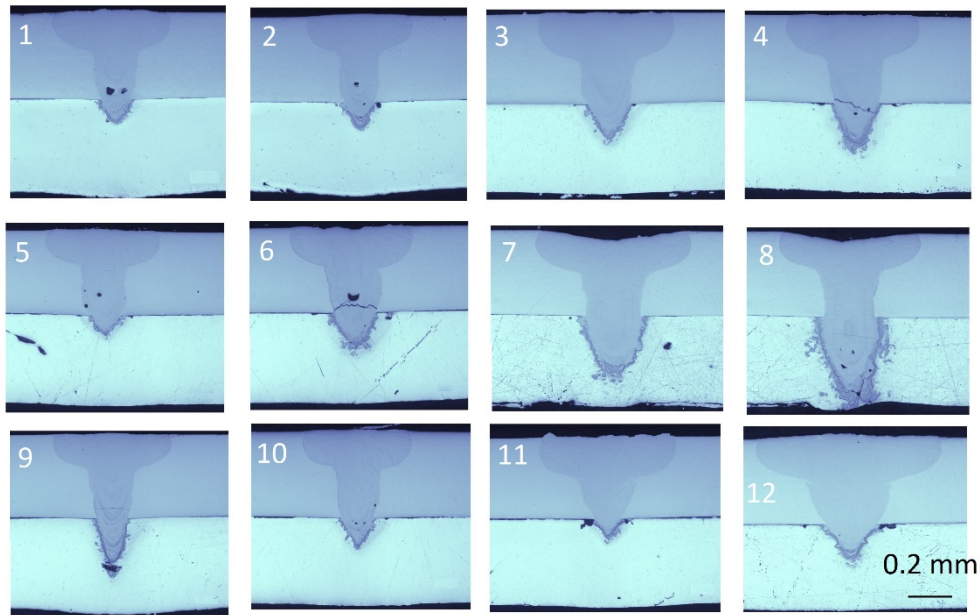


Fig. 4. Cross sections of laser welded dissimilar joint of stainless steel 316L and aluminium alloy A1050; sample numbers are correlated with data presented in Table 1.

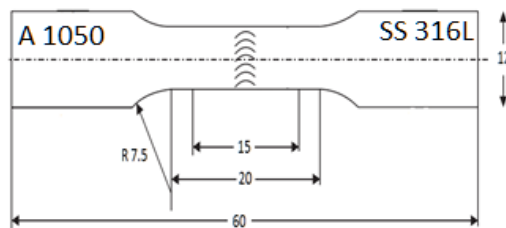


Fig. 5. Schematic representation of the specimen for tensile strength.

Results on the tensile strength of dissimilar welding, for the selected samples, are presented in table 3. The standard force as a function of elongation is presented in figure 6. The strongest weld is also the one without defects, as it can be observed from the figure 4 and the table 3. This can be identified as the third specimen, which was obtained using 0.5 m/min speed at the focus position.

Table 3

Tensile tests results

Legend	Specimen	$R_{p0.2}$ [MPa]	R_m [MPa]	F_m [kN]
	3	50	55.3	0.38
	7	40	46	0.32
	8	-	-2.49	-0.01

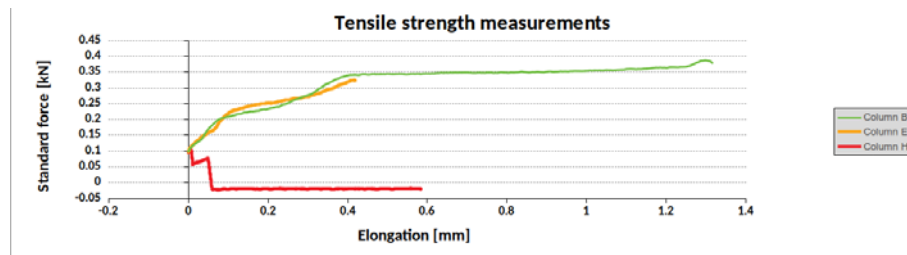


Fig. 6. Graphic representation of the tensile strength

3.3. Scanning Electron Microscope Evaluation

The sample which was determined to yield best results after metallographic analysis, as well as in terms of mechanical resistance to breaking, was chosen for electron microscopy analysis. This is done in order to validate the results of previous examinations. Two cracks with an approximate size of 100 μm near SS316L alloy side can be observed in figure 6.

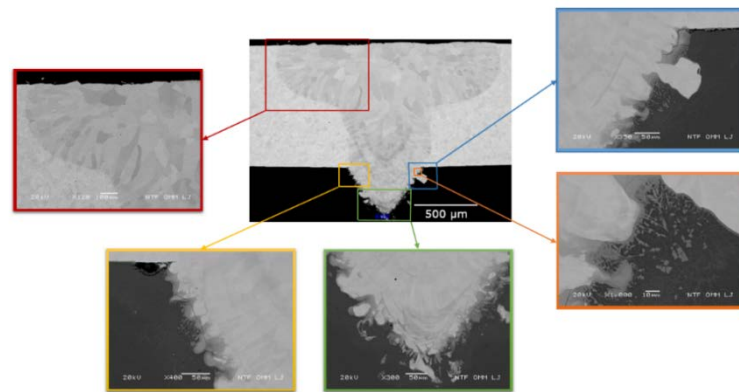


Fig. 6. SEM Evaluation of the cross-section of sample 3.

For samples 3 and 8, with parameters presented in table 2, the focus position is lowered into the sample. However, the energy density at the surface of the sample is sufficient in order to initiate the welding process. As the material melts and mixes, therefore the laser-matter interaction moving deeper into the sample, the energy density increases with depth, which sustains the welding process deeper into the sample. This process results in a higher penetration depth.

4. Conclusions

In this study, dissimilar welding in a lap joint configuration was investigated. The utilized materials are stainless steel 316L and aluminium A1050 ($t=1\text{mm}$). Laser welding was conducted using a fiber laser with 400 W maximum power. The welded samples were analysed using metallographic examination to

determine the weld depth and defects. SEM was used to validate the results of metallographic evaluation, while the tensile strength tests characterize the mechanical properties.

Results presented in this paper can be summarized as follows:

- ✓ Highest tensile strength was achieved when a small part of stainless steel, approximate 200 μm , melted into aluminium.
- ✓ Cracks and defects appear proportionally to the welding depth
- ✓ According to the metallographic examination, best results are obtained using a scan speed of 0.5 m/min and -2 mm defocus.

Acknowledgements

This work was supported by the COST Action MP1401: Advanced fibre laser and coherent source as tools for society, manufacturing and life-science. Part of the research done by the Romanian team was performed at the CETAL laser facility, and was financed by the National Authority for Research and Innovation in the frame of “Nucleus” programme, under the contract 4N/2015.

We would also like to thank Yaskawa Slovenia for supplying their commercially available robotic system for remote laser welding applications. The Slovenian authors acknowledge the financial support from the state budget by the Slovenian Research Agency (Programmes No. P2-0392 and P2-0270).

REFERENCES

- [1] *M. Zamfirescu, M. Ulmeanu, F. Jipa, I. Anghel, S. Simion, R. Dabu, I. Ionita*, “Laser processing and characterization with femtosecond laser pulses”, *Romanian Reports In Physics*, **vol. 62**, 594, (2010).
- [2] *M. Stafe, I. Vlădoiu, C. Negutu, I. M. Popescu*, “Experimental investigation of the nanosecond laser ablation rate of aluminum”, *Romanian Reports In Physics*, **vol. 60**, 789 (2008).
- [3] *M. Stafe, C. Negutu, N. N. Puscas, I. M. Popescu*, “Pulsed laser ablation of solids”, *Romanian Reports In Physics*, **vol. 62**, 758 (2010).
- [4] *V.G. Niziev and A.V. Nesterov*, “Influence Of Beam Polarization On Laser Cutting Efficiency”, *Journal Of Physics D: Applied Physics*, **vol. 32**, 1455 (1999).
- [5] *K.-M. Hong, Y. C. Shin*, “Prospects Of Laser Welding Technology In The Automotive Industry: A Review”, *Journal Of Materials Processing Technology*, **vol. 245**, 46 (2017).
- [6] *X. Xu, G. Mi, Y. Luo, P. Jiang, X. Shao, C. Wang*, “Morphologies, Microstructures, And Mechanical Properties Of Samples Produced Using Laser Metal Deposition With 316L Stainless Steel Wire”, *Optics And Lasers In Engineering*, **vol. 94**, 1 (2017).
- [7] *J. Sun, Q. Yan, W. Gao, J. Huang*, “Investigation Of Laser Welding On Butt Joints Of Al/Steel Dissimilar Materials, *Materials & Design*”, **vol. 83**, 120 (2015).
- [8] *O. Seffer, R. Pfeifer, A. Springer, S. Kaierle*, “Investigations On Laser Beam Welding Of Different Dissimilar Joints Of Steel And Aluminium Alloys For Automotive Lightweight Construction”, *Physics Procedia*, **vol. 83**, 383 (2016).
- [9] *Y. Ai, X. Shao, P. Jiang, P. Li, Y. Liu, W. Liu*, “Welded Joints Integrity Analysis And Optimization For Fiber Laser Welding Of Dissimilar Of Dissimilar Materials”, *Optics And Lasers In Engineering*, **vol. 86**, 62 (2016).